Journal of Organometallic Chemistry 696 (2011) 2904–2909

Contents lists available at ScienceDirect

Journal of Organometallic Chemistry

journal homepage: www.elsevier.com/locate/jorganchem

The reactions of $Ir(CO)Cl(PPh_3)_2$ with $HSnPh_3$

Richard D. Adams*, Fang Fang, Mark D. Smith, Qiang Zhang

Department of Chemistry and Biochemistry, University of South Carolina, Columbia, SC 29208, United States

ARTICLE INFO

Article history:
Received 9 February 2011
Received in revised form
11 March 2011
Accepted 23 March 2011

Keywords:
Oxidative addition
Vaska's compound
Iridium
Tin

ABSTRACT

A reinvestigation of the reaction of $Ir(CO)Cl(PPh_3)_2$, **1** with $HSnPh_3$ has revealed that the oxidative-addition product $Ir(CO)Cl(PPh_3)_2(H)(SnPh_3)$, **2** has the H and $SnPh_3$ ligands in cis-related coordination sites. Compound **2** reacts with a second equivalent of $HSnPh_3$ by a Cl for H ligand exchange to yield the new compound $H_2Ir(CO)(SnPh_3)(PPh_3)_2$, **3**. Compound **3** contains two cis- related hydride ligands. Under an atmosphere of CO, **1** reacts with $HSnPh_3$ to replace the Cl ligand with $SnPh_3$ and one of the PPh_3 ligands with a CO ligand and also adds a second equivalent of CO to yield the 5-coordinate complex $Ir(CO)_3(SnPh_3)(PPh_3)$, **4**. Compound **4** reacts with $HSnPh_3$ by loss of CO and oxidative addition of the Sn-H bond to yield the 6-coordinate complex $HIr(CO)_2(SnPh_3)_2(PPh_3)$, **5** that contains two trans-positioned $SnPh_3$ ligands.

1. Introduction

In recent years we have been investigating the synthesis of polynuclear transition metal complexes containing phenyl-substituted tin ligands from reactions of metal carbonyl complexes with phenylstannanes, e.g. eqs. (1)–(3) [1–5].

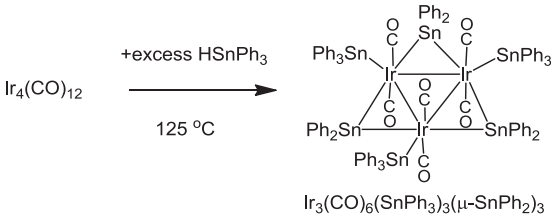

(1)

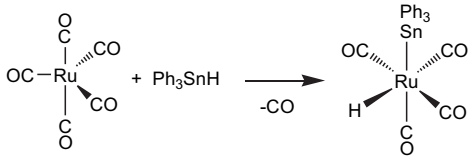

(2)

Recent studies have shown that clusters such as these can serve as precursors to catalysts that exhibit improved selectivity for certain types of hydrogenation reactions [5–8]. Because all of the metal atoms in reactions (1)–(3) have 18 electron configurations, these reactions occur by a combination of CO elimination and oxidative addition of the Sn–H bond to the transition metal atoms. Cleavage of phenyl groups from the tin atom often leads to the formation of benzene by combination with a hydride ligand and simultaneous formation of a bridging $SnPh_2$ ligand from the remainder of the tin ligand, eqs. (1) and (3). Reactions of tertiary stannanes with unsaturated metal complexes frequently involve only the oxidation addition step of the SnH bond to the metal atom, e.g. eq. (4) [9]. One of the classic examples is the reaction of Vaska's compound [10]

$Ir(CO)Cl(PPh_3)_2$, **1** with $HSnPh_3$. This reaction was first reported by Lappert et al. in 1968, eq. (5) [11]. Most oxidative addition reactions to **1** proceed to give *cis* addition products, but on the basis of spectroscopic data and comparisons to related compounds, Lappert et al. proposed a structure for the product $Ir(CO)Cl(PPh_3)_2(H)(SnPh_3)$, **2** that had the H and $SnPh_3$ ligands in *trans*-coordination sites, as shown for the structure **A**, eq. (5).

Because of the fundamental importance of the Sn-H oxidative-addition reaction to our work, we have reinvestigated the reaction of **1** with $HSnPh_3$. We have found that the reaction of **1** with $HSnPh_3$ is richer than originally reported and the stereochemistry **A** that was originally-proposed for the structure of **2**, is, in fact, incorrect. The results of our study of these reactions are described in this report.

* Corresponding author.
E-mail address: Adams@chem.sc.edu (R.D. Adams).

0022-328X/$ – see front matter © 2011 Elsevier B.V. All rights reserved.
doi:10.1016/j.jorganchem.2011.03.030

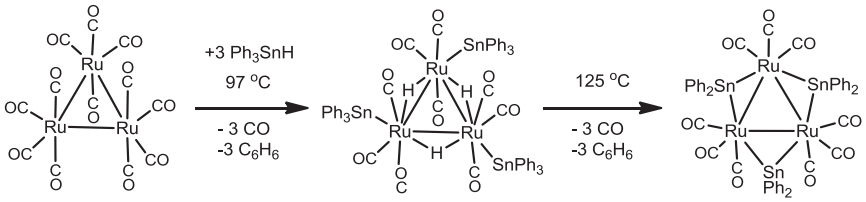

(3)

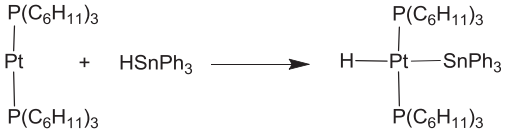

(4)

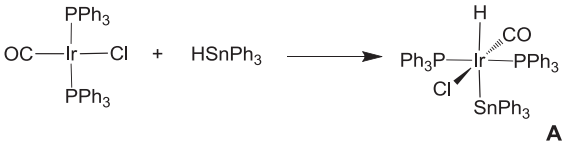

(5)

2. Experimental section

General Data - All reactions were performed either under nitrogen or under a carbon monoxide atmosphere as specified below by using standard Schlenk techniques. Reagent grade solvents were dried by the standard procedures and were freshly distilled under nitrogen prior to use. Infrared spectra were recorded on a Thermo-Nicolet Avatar 360 FT-IR spectrophotometer. ^{1}H NMR spectra were recorded on Mercury 300 spectrometer operating at 300.1 MHz and Mercury 400 spectrometer operating at 399.9 MHz ^{31}P{^{1}H} NMR were recorded on a Varian Mercury 500 spectrometer operating at 202.486 MHz. Mass spectral (MS) measurements performed by a using direct-exposure probe using electron impact (EI) or electrospray (ES) ionizations were made on a VG 70S instrument. Product separations were performed by TLC in the open air on Analtech 0.25 or 0.5 mm silica gel 60 Å F_{254} glass plates. $Ir(CO)Cl(PPh_3)_2$, **1** was purchased from STREM and was used without further purification. $HSnPh_3$, Ph_3SnCl and $LiAlD_4$ were purchased from Aldrich and were used without further purification.

2.1. Synthesis of $HIrCl(CO)(SnPh_3)(PPh_3)_2$, 2

A 50.0 mg amount **1** (0.062 mmol) was dissolved in 30 mL of CH_2Cl_2 in a 100 mL three-neck flask to form a yellow solution. The reaction flask was evacuated and refilled with nitrogen. 23.0 mg of $HSnPh_3$ (0.065 mmol) was then added to the flask. The solution immediately turned from yellow to colorless. The solution allowed to stir for 15 min at room temperature and was then concentrated by purging with nitrogen. Colorless crystals formed when the concentrated reaction solution was cooled to −20 °C. 40 mg of colorless crystals of **2** (52% yield) were collected. Spectral data for $HIrCl(CO)(SnPh_3)(PPh_3)_2$, **2**: IR (cm^{-1} in CH_2Cl_2): 2014(w, ν_{Ir-H}), 2004(m, ν_{CO}). ^{1}H NMR (in $CDCl_3$): δ = 6.96–7.37 (m, 45H, Ph), δ = −8.12 (dd, hydride, $^2J_{P1-Hcis}$ = 14.71 Hz, $^2J_{P2-Htrans}$ = 146.15 Hz). Mass Spectrum: EI-MS showed the parent ion at m/z 1105 (M^+−CO).

2.2. Synthesis of $H_2Ir(CO)(SnPh_3)(PPh_3)_2$, 3

A 30.0 mg amount **1** (0.038 mmol) was dissolved in 15 mL of CH_2Cl_2 in a 100 mL three-neck flask. The flask was then evacuated and refilled with nitrogen, then 68.0 mg $HSnPh_3$ (0.194 mmol) was added to the solution. The solution immediately turned from yellow to colorless. After stirring for 7 h, the solvent was removed in vacuo. The residue was washed with hexane twice and then redissolved in CH_2Cl_2 to form a suspension. After separated by filtration, the solution was concentrated to 1 mL. Then 10 mL hexane was added to this solution as precipitant. The mixture was allowed to stay at −20 °C for 30 min to make sure the precipitation was complete. The white precipitate was collected by filtration and washed with hexane again to yield 15.3 mg (37% yield) of $H_2Ir(CO)(SnPh_3)(PPh_3)_2$, **3**. Side products of this reaction are $O{=}PPh_3$ (3.2 mg; 18%) and $SnPh_4$ (2.6 mg; 8%). Spectral data for **3**: IR (cm^{-1} in CH_2Cl_2): 2071(m, ν_{Ir-H}), 1965(m, ν_{CO}). ^{1}H NMR (in CD_2Cl_2): δ = 6.85–7.22 (m, 45H, Ph), −11.42 (ddd, hydride, $^2J_{P2-H1}$ = 16.40 Hz, $^2J_{P1-H1}$ = 99.98 Hz, $^1J_{H2-H1}$ = 4.40 Hz) and −10.430 (ddd, hydride, $^2J_{P-H1}$ = 19.20 Hz and 14.80Hz, $^1J_{H1-H2}$ = 4.80 Hz). ^{31}P NMR (in $CDCl_3$): δ = 7.36 (d, P2, $^2J_{P2-P1}$ = 9.9 Hz, $^2J_{P2-119Sn}$ = 1162 Hz, $^2J_{P2-117Sn}$ = 1120 Hz); 4.11 (d, P1, $^2J_{P2-P1}$ = 9.9 Hz, $^2J_{P2-119Sn}$ = $^2J_{P2-117Sn}$ = 89 Hz) Mass Spectrum: EI-MS showed the parent ion at m/z = 1096.

2.3. Synthesis of $D_2Ir(CO)(SnPh_3)(PPh_3)_2$, 3-$d_2$

A 88.0 mg amount of Ph_3SnCl (0.228 mmol) was dissolved in 30 mL of ethyl ether in a 250 mL three-neck flask. To this solution, 15 mg $LiAlD_4$ (0.357 mmol) was added and stirred for 20 h under N_2. The solvent was then removed in vacuo. The product was collected by sublimation by heating the residue to 170 °C at 0.3 mm Hg for 2h. 46.6 mg $DSnPh_3$ was collected by sublimation onto a cold finger. This procedure is similar to that used by Wittig who used triphenyltin bromide [12]. A 30.0 mg amount of **1** (0.038 mmol) was dissolved in 20 mL of CH_2Cl_2 in a 100 mL three-neck flask. The flask was evacuated and refilled with nitrogen, then 46.0 mg $DSnPh_3$ (0.131 mmol) was added, and the solution was stirred for 20 h. The solvent was then removed in vacuo, the products were separated by TLC by using 4:1 hexane-methylene chloride solvent mixture to yield 0.8 mg (2% yield) of **3-d$_2$**. Spectral data for **3-d$_2$**: IR ν_{CO} (cm^{-1} in CH_2Cl_2): 1996(m).

2.4. Synthesis of $Ir(CO)_3(SnPh_3)(PPh_3)$, 4 and $HIr(CO)_2(SnPh_3)_2(PPh_3)$, 5

A 25.0 mg amount of **1** (0.032 mmol) was dissolved in 20 mL of CH_2Cl_2 in a 100 mL three-neck flask. The flask was evacuated and refilled with nitrogen. 28.0 mg $HSnPh_3$ (0.080 mmol) was added to the flask and then CO gas was slowly purged through the solution for 20 h. After the solvent was removed in vacuo, the products were separated by TLC by using 4:1 hexane-methylene chloride solvent mixture to yield in order of elution: 9.3 mg of $Ir(CO)_3(SnPh_3)(PPh_3)$ **4** (12% yield) and 2.5 mg of **5** (6.5% yield). Spectral data for **4**: IR ν_{CO} (cm^{-1} in CH_2Cl_2): 1965(s), 2028(vw). ^{1}H NMR (in $CDCl_3$): δ = 7.23–7.64 (m, 30H, Ph). Mass Spectrum: ES-MS showed the parent ion at m/z 889 (M + H). Spectral data for **5**: IR ν_{CO} (cm^{-1} in CH_2Cl_2): 1963(m), 2005(s), 2058(vw). ^{1}H NMR (in $CDCl_3$): δ = 6.91–7.48 (m, 45H, Ph), δ = −10.97 (d, hydride, $^2J_{P-H}$ = 89.73 Hz). Mass Spectrum: EI-MS showed the parent ion M^+ at m/z 1212.

2.4.1. Conversion from 4 to 5

A 16 mg amount of **4** (0.018 mmol) was dissolved in 15 mL of CH_2Cl_2 in a 100 mL three-neck flask under a nitrogen atmosphere. To this solution, 7.0 mg of $HSnPh_3$ (0.020 mmol) was added and stirred for 12 h. The solvent was then removed in vacuo, the products were separated by TLC by using 4:1 hexane-methylene chloride solvent mixture to yield 17.3 mg (78% yield) of **5**.

2.4.2. Conversion from 2 to 3

A 21.8 mg amount of **2** (0.019 mmol) was dissolved in 15 mL of CH_2Cl_2 in a 100 mL three-neck flask under a nitrogen atmosphere. To this solution, 35.0 mg of $HSnPh_3$ (0.100 mmol) was added and stirred for 3 h to yield 10.6 mg (51% yield) of **3.**

3. Crystallographic analyses

Colorless single crystals of **2** suitable for x-ray diffraction analysis were obtained by slow evaporation of solvent from the reaction solutions in methylene chloride/hexane solvent mixtures by cooling to −20 °C. Colorless single crystals **3**, **4** and **5** suitable for x-ray diffraction analyses were obtained by slow evaporation of solvent from solutions in methylene chloride/hexane solvent mixtures at room temperature. Each data crystal was glued onto the end of a thin glass fiber. X-ray intensity measurements were performed by using a Bruker SMART APEX CCD-based diffractometer using Mo Kα radiation ($\lambda = 0.71073$ Å). The raw data frames were integrated with the SAINT + program by using a narrow-frame integration algorithm [13]. Corrections for Lorentz and polarization effects were also applied with SAINT+. An empirical absorption correction based on the multiple measurement of equivalent reflections was applied by using the program SADABS [13]. All structures were solved by a combination of direct methods and difference Fourier syntheses, and refined on F^2 by full-matrix least-squares by using the SHELXTL software package [14]. All non-hydrogen atoms were refined with anisotropic thermal parameters. All hydrogen atoms on the ligands were placed in geometrically idealized positions and included as standard riding atoms during the least-squares refinements. Crystal data, data collection parameters, and results of the analyses are listed in Table 1.

Compound **2** crystallized in the trigonal crystal system. The space group $P3_2$ was used to begin the structure solution and refinement. In the final stages of the refinement it was found that the crystal was a twin. The twin law, 0 1 0/1 0 0/0 0 -1, was established which was combined with an inversion operator to generate four domains. The two domains corresponding to space group $P3_2$ constitute a volume fraction of 0.640(5). The crystal of **2** contains one independent formula equivalent of the complex and one formula equivalent of CH_2Cl_2 from the crystallization solvent in the asymmetric unit. Compound **3** crystallized in the triclinic crystal system. The space group $P\bar{1}$ was assumed and confirmed by the successful solution and refinement of the structure. Compound **4** crystallized in the monoclinic crystal system. The space group $P2_1/c$ was established by the systematic absences in the data and confirmed by the successful solution and refinement of the structure. Compound **5** crystallized in the monoclinic crystal system. The space group and setting $P2_1/n$ was established by the systematic absences in the data and confirmed by the successful solution and refinement of the structure. The hydrido ligand in the analysis of compound **2** was located and refined with the restraint, Ir−H = 1.80 Å. The hydrido ligands in the analysis of compound **3** were both located in credible positions in difference Fourier syntheses. Only H(1) could be refined to convergence. The second one H(2) was included as a fixed contribution in the final refinements. The hydrido ligand in **5** was located in a difference Fourier synthesis and was subsequently refined to convergence.

4. Results and discussion

$HIrCl(CO)(SnPh_3)(PPh_3)_2$, **2** was obtained in 52% yield from the reaction of **1** with $HSnPh_3$ at room temperature. As mentioned above, this compound was reported initially in 1968 [11]. Our IR spectra of **2** are similar to that which was reported then. However, unlike the previous study we have performed a complete single-crystal X-ray diffraction analysis of the compound in order to determine its molecular structure. An ORTEP diagram of the molecular structure of **2** is shown in Fig. 1. The structure has a distorted octahedral arrangement of the six ligands. However, the stereochemistry **B** differs from that proposed by Lappert structure

Table 1
Crystallographic data for compounds 2 - 5.

Compound	2	3	4	5
Empirical formula	$IrSnP_2ClC_{55}H_{46}O \cdot CH_2Cl_2$	$IrSnP_2C_{55}H_{47}O$	$IrSnPC_{39}H_{30}O_3$	$IrSn_2PC_{56}H_{46}O_2$
Formula weight	1216.12	1096.76	888.49	1211.48
Crystal system	Trigonal	Triclinic	Monoclinic	Monoclinic
Lattice parameters				
a (Å)	12.7726(2)	10.4816(3)	14.963(4)	11.9977(7)
b (Å)	12.7726(2)	12.6526(4)	12.218(3)	12.6738(7)
c (Å)	26.6872(6)	18.2048(6)	19.909(5)	32.5152(18)
α (deg)	90.00	78.200(1)	90.00	90.00
β (deg)	90.00	84.827(1)	108.045(5)	97.094(1)
γ (deg)	120.00	87.998(1)	90.00	90.00
V (Å^3)	3770.44(12)	2353.33(13)	3460.6(14)	4906.3(5)
Space group	$P3_2$	$P-1$	$P2_1/c$	$P2_1/n$
Z value	3	2	4	4
ρ_{calc} (g/cm^3)	1.607	1.548	1.705	1.640
μ (Mo K_α) (mm^{-1})	3.403	3.461	4.645	3.788
Temperature (K)	294(2)	294(2)	294(2)	294(2)
$2\Theta_{max}$ (°)	52.74	50.06	50.06	50.06
No. Obs. ($I > 2\sigma(I)$)	10254	8310	6117	8667
No. Parameters	607	545	406	563
Goodness of fit GOF[a]	1.097	1.073	1.062	1.089
Max. shift in cycle	0.002	0.002	0.001	0.001
Residuals[a]: R1; wR2	0.0278, 0.0549	0.0279, 0.0648	0.0312, 0.0802	0.0446, 0.0771
Absorption Correction, Max/min	Multi-scan 1.000/0.621	Multi-scan 1.000/0.866	Multi-scan 1.000/0.632	Multi-scan 1.000/0.831
Largest peak in Final Diff. Map (e$^-$/Å^3)	1.000	2.923	0.825	0.615

[a] $R = \Sigma_{hkl}(||F_{obs}|-|F_{calc}||)/\Sigma_{hkl}|F_{obs}|$; $R_w = [\Sigma_{hkl}w(|F_{obs}|-|F_{calc}|)^2/\Sigma_{hkl}wF_{obs}^2]^{1/2}$, $w = 1/\sigma^2(F_{obs})$; $GOF = [\Sigma_{hkl}w(|F_{obs}|-|F_{calc}|)^2/(n_{data}-n_{vari})]^{1/2}$.

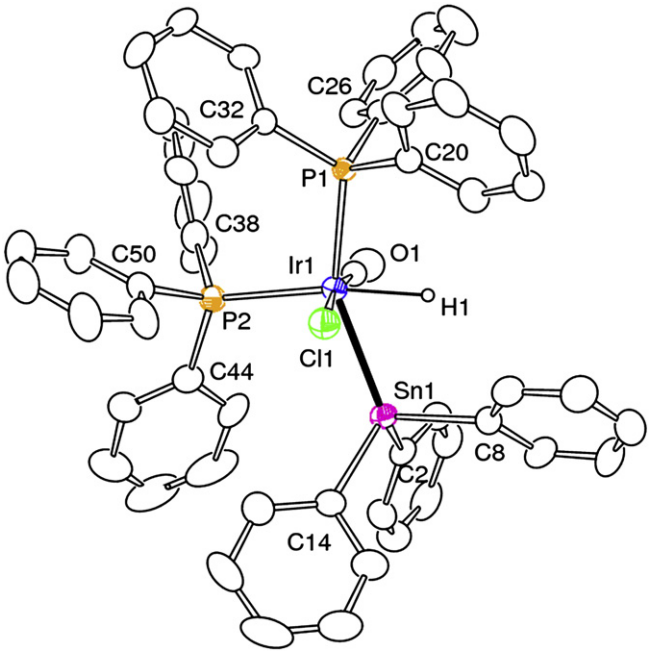

Fig. 1. ORTEP diagram of the molecular structure of compound 2 showing 30% probability thermal ellipsoids. The hydrogen atoms on the phenyl rings are omitted for clarity. Selected interatomic bond distances (Å) and angles (°) are as follow: Ir(1) - Sn(1) = 2.6455(6), Ir(1) - P(1) = 2.4022(18), Ir(1)–P(2) = 2.4525(19), Ir(1)–C(1) = 1.865(10), Ir(1)–Cl(1) = 2.4185(18), Ir(1)–H(1) = 1.806(10); P(1)–Ir(1) - Cl(1) = 86.64(6), C(1)–Ir(1)–P(2) = 89.6(2), C(1)–Ir(1)–Cl(1) = 170.4(2), P(1)–Ir(1)–P(2) = 102.91(6), Cl(1)–Ir(1)–P(2) = 97.42(6), C(1)–Ir(1)–Sn(1) = 90.4(2), P(1)–Ir(1)–Sn(1) = 150.67(4), Cl(1)–Ir(1)–Sn(1) = 81.46(5), P(2)–Ir(1)–Sn(1) = 105.13(4), P(1)–Ir(1)–H(1) = 89(3), P(2)–Ir(1)–H(1) = 164(3).

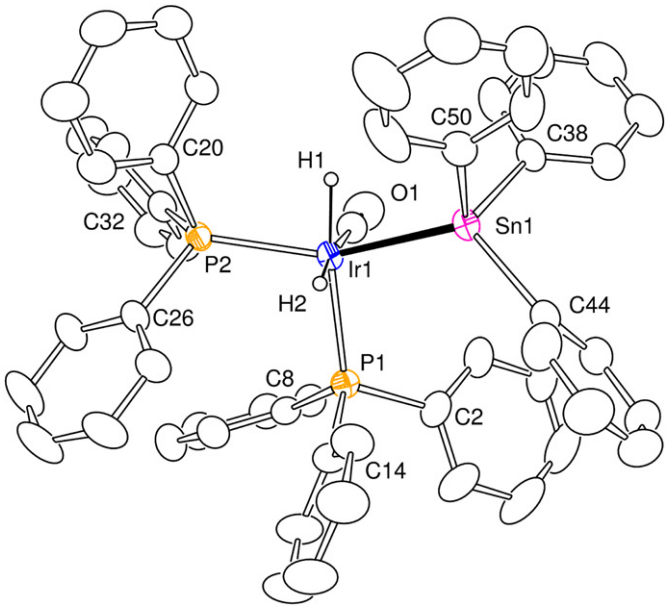

Fig. 2. ORTEP diagram of the molecular structure of compound 3 showing 30% probability thermal ellipsoids. The hydrogen atoms on the phenyl rings are omitted for clarity. Selected interatomic bond distances (Å) and angles (○) are as follow: Ir(1) - Sn(1) = 2.6259(3), Ir(1) - P(1) = 2.3567(10), Ir(1)–P(2) = 2.3290(10), Ir(1)–C(1) = 1.914(5), Ir(1)–H(1) = 1.38(6), Ir(1) - H(2) = 1.69; C(1)–Ir(1)–P(2) = 100.40(14), C(1)–Ir(1)–P(1) = 92.21(14), P(2)–Ir(1)–P(1) = 104.99(4), C(1)–Ir(1)–Sn(1) = 98.28(14), P(2)–Ir(1)–Sn(1) = 147.52(3), P(1)–Ir(1)–Sn(1) = 100.57(3).

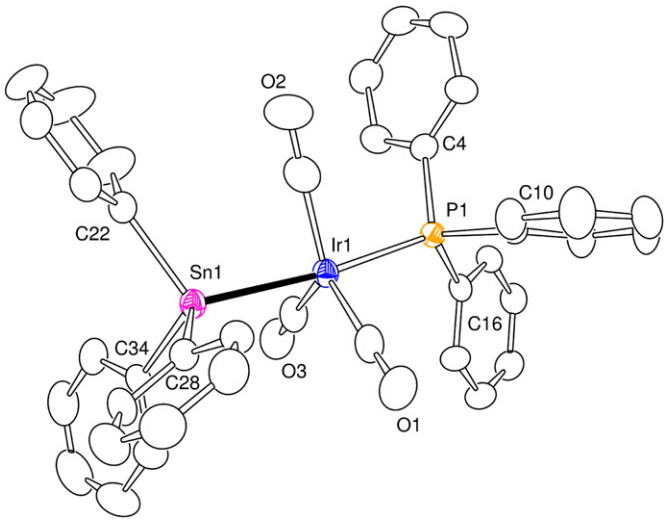

Fig. 3. ORTEP diagram of the molecular structure of compound 4 showing 30% probability thermal ellipsoids. The hydrogen atoms on the phenyl rings are omitted for clarity. Selected interatomic bond distances (Å) and angles (○) are as follow: Ir(1) - Sn(1) = 2.6629(7),, Ir(1) - P(1) = 2.3522(13), Ir(1)–C(1) = 1.913(6), Ir(1)–C(3) = 1.921(6), Ir(1)–C(2) = 1.921(8); P(1)–Ir(1)–Sn(1) = 173.80(3).

A in that the two PPh_3 ligands in **2** occupy *cis* related sites and the $SnPh_3$ and H ligands also occupy *cis* related sites.

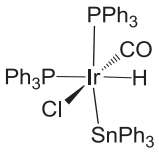

The P(1)–Ir(1) – P(2) angle is 102.91(6)°. The CO and Cl ligands are *trans* related, C(1)–Ir(1)–Cl(1) = 170.4(2)°. The $SnPh_3$ ligand is significantly displaced away from the phosphine P(2) toward the hydride ligand H(1), P(2)–Ir(1)–Sn(1) = 105.13(4)°, P(1)–Ir(1)–

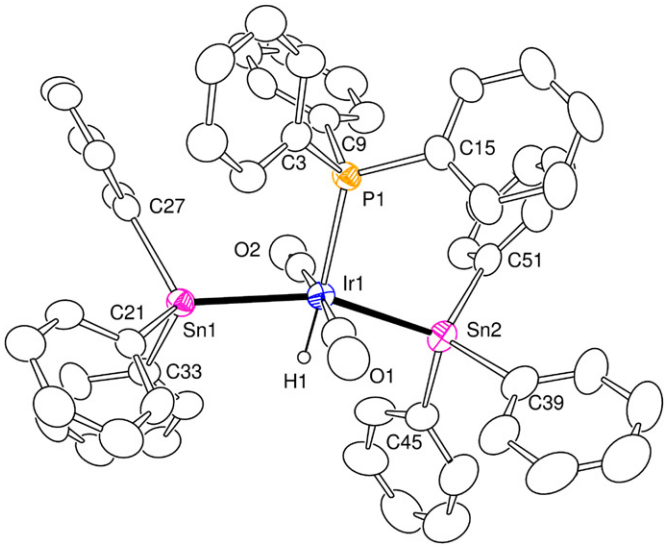

Fig. 4. ORTEP diagram of the molecular structure of compound 5 showing 30% probability thermal ellipsoids. The hydrogen atoms on the phenyl rings are omitted for clarity. Selected interatomic bond distances (Å) and angles (○) are as follow: Ir(1)-Sn(1) = 2.6649(5), Ir(1)-Sn(2) = 2.6744(6), Ir(1)–P(1) = 2.3805 (18), Ir(1)–C(1) = 1.874(8), Ir(1)–C(2) = 1.905(9), Ir(1)–H(1) = 1.27(5); Sn(1)–Ir(1)–Sn(2) = 153.76(2), P(1)–Ir(1)–Sn(1) = 102.76(5), P(1)–Ir(1)–Sn(2) = 101.70(5), C(1)–Ir(1)–C(2) = 174.9(3).

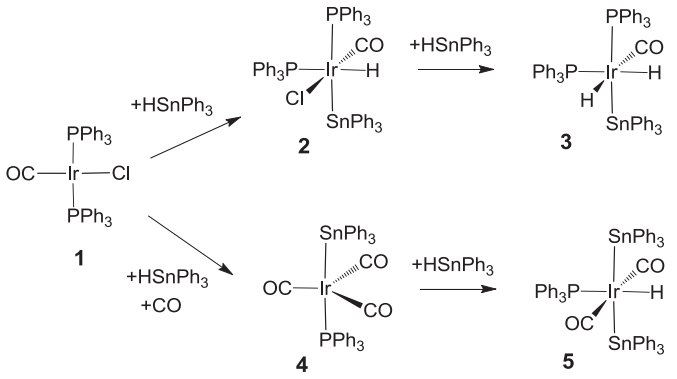

Scheme 1.

Sn(1) = 150.68(4)°. This distortion is probably of a steric origin. The Ir–Sn bond distance, Ir(1) - Sn(1) = 2.6455(6) Å, is slightly longer than the Ir–Sn distance, 2.6216(5) Å, that we observed in the less-crowded 5-coordinate complex $Ir(COD)(CO)_2SnPh_3$, **6** [15]. The hydride ligand was located in a difference Fourier synthesis and refined by using the restraint, Ir–H = 1.80 Å. The hydride exhibits the characteristic high-field resonance shift in the ^1H NMR spectrum, $\delta = -8.12$ with suitable couplings to the *cis* and *trans* related phosphine ligands, $^2J_{P1-Hcis} = 14.71$ Hz, $^2J_{P2-Htrans} = 146.15$ Hz.

When compound **1** was allowed to react with 5 equivalents of $HSnPh_3$, the new compound $H_2Ir(CO)(SnPh_3)(PPh_3)_2$, **3** was obtained in 37% yield. Compound **3** was also obtained in 51% yield from a reaction of **2** with $HSnPh_3$ at room temperature. An ORTEP diagram of the molecular structure of **3** is shown in Fig. 2. Compound **3** differs from **2** in that the Cl ligand has been replaced by a hydride ligand. We and others have shown that $HSnPh_3$ will react with certain metal halide complexes including those of iridium to substitute the halide ligand with a $SnPh_3$ ligand [15]. Like **2**, compound **3** also has a distorted octahedral arrangement of its six ligands. As in **2**, the two PPh_3 ligands are *cis*-related, P(2)–Ir(1)–P(1) = 104.99(4)°. There are two *cis*-related hydride ligands with appropriate couplings to each other and to the phosphine ligands, $\delta = -11.42$ (ddd, hydride, $^2J_{P2-H1} = 16.40$ Hz, $^2J_{P1-H1} = 99.98$ Hz, $^1J_{H2-H1} = 4.40$ Hz) and −10.430 (ddd, hydride, $^2J_{P-H1} = 19.20$ Hz and 14.80Hz, $^1J_{H1-H2} = 4.80$ Hz). The $SnPh_3$ ligand lies *cis* to the two hydride ligands *cis* to one PPh_3 ligand, P(1)–Ir(1)–Sn(1) = 100.57(3)°, and approximately *trans* to the other, P(2)–Ir(1)–Sn(1) = 147.52(3)°. The Ir–Sn bond distance is slightly shorter than that in **2**, Ir(1) - Sn(1) = 2.6259(3) Å. The IR spectrum exhibits two absorptions in the CO stretching region, 2071 cm^{-1}, 1965 cm^{-1}. The absorption at 2071 cm^{-1} is due to the hydride ligands. This was confirmed by synthesizing the dideuteride compound **3-d₂**. **3-d₂** shows only the CO absorption at 1996 cm^{-1}. The difference in the position of the CO absorption between **3** and **3-d₂** is due to the effects of coupling of the hydride vibration to the CO vibration in **3** [16].

When compound **1** was allowed to react with $HSnPh_3$ under an atmosphere of CO, two new compounds $Ir(CO)_3(SnPh_3)(PPh_3)$, **4** and $HIr(CO)_2(SnPh_3)_2(PPh_3)$, **5** were formed in low yields. Both products were characterized by IR, ^1H NMR, mass spec and single crystal X-ray diffraction analyses. An ORTEP diagram of the molecular structure of **4** is shown in Fig. 3. Compound **4** has a trigonal bipyramidal structure with three terminal carbonyl ligands in the equatorial plane and one PPh_3 ligand and one $SnPh_3$ ligand in the axial sites, P(1)–Ir(1)–Sn(1) = 173.80(3)°. The Ir–Sn bond distance, Ir(1) - Sn(1) = 2.6629(7) Å, is slightly longer than those in **2**, **3**, **6** and those in the anion $[Ir(CO)_3(SnPh_3)_2]^-$, Ir–Sn = 2.6284(4) Å and 2.6289(4) Å [17], but is very similar to the Ir–Sn distance, 2.6610(3) Å, found for the similar compound $Ir(CO)_3(SnPh_3)[P(cyclo\text{-}C_6H_{11})]_3$ [18].

An ORTEP diagram of the molecular structure of **5** is shown in Fig. 4. Compound **5** contains six ligands: two $SnPh_3$, one PPh_3, two CO ligands and one hydride arranged in an octahedral-like geometry. The two $SnPh_3$ ligands are *trans* to one another, but are displaced toward the hydride ligand, Sn(1)–Ir(1)–Sn(2) = 153.76(2)°. The Ir - Sn distances, Ir(1) - Sn(1) = 2.6649(5) Å, Ir(1) - Sn(2) = 2.6744(6) Å are similar to that in **4**. The hydride ligand was located and refined in the analysis and lies *trans* to the PPh_3 ligand, $\delta = -10.97$ ($^2J_{P-H} = 89.73$ Hz). The refined Ir(1)–H(1) distance 1.27(5) Å is a little shorter than expected, but the standard deviation is large due to the low scattering power of hydrogen relative to that of iridium. The CO ligands lie trans to one another, C(1)–Ir(1)–C(2) = 174.9(3)°. Compound **4** can be converted to **5** in 78% yield by a reaction with $HSnPh_3$ that is accompanied with a loss of CO.

5. Summary

The reactions and products reported here are shown in Scheme 1. If was found that the reaction of **1** with $HSnPh_3$ yields the oxidative addition product **2** which has a *cis* stereochemistry of the $SnPh_3$ and H ligands on the iridium atom. Compound **2** reacts with a second equivalent of $HSnPh_3$ by a Cl for H exchange to yield the product **3** that contains two *cis*-related hydride ligands.

Under an atmosphere of CO, compound **1** reacts with $HSnPh_3$ to replace the Cl ligand with $SnPh_3$ and one of the PPh_3 ligands with a CO ligand and also adds a second equivalent of CO to yield the 5-coordinate 18 electron iridium (I) complex **4**. The mechanism of the formation of **4** was not established in this work. Compound **4** reacts with $HSnPh_3$ by loss of CO and oxidative addition of the Sn-H bond to yield the 6-coordinate 18 electron iridium (III) complex **5** that contains two *trans*-positioned $SnPh_3$ ligands.

Acknowledgements

This research was supported by the National Science Foundation under Grant No. CHE-0743190. We thank the USC NanoCenter for partial support of this work.

Appendix A. Supplementary Material

CCDC 812194–812197 contain the supplementary crystallographic data for compounds **2**–**5**. These data can be obtained free of charge from the Cambridge Crystallographic Data Centre via www.ccdc.cam.ac.uk/data_request/cif.

References

[1] R.D. Adams, B. Captain, J.L. Smith Jr., Inorg. Chem. 43 (2004) 7576–7578.
[2] R.D. Adams, E. Trufan, Phil. Trans. Royal Soc. 368 (2010) 1473–1493.
[3] R.D. Adams, B. Captain, E. Trufan, L. Zhu, J. Am. Chem. Soc. 129 (2007) 7545–7556.
[4] R.D. Adams, B. Captain, E. Trufan, J. Organomet. Chem. 693 (2008) 3593–3602.
[5] R.D. Adams, E.M. Boswell, B. Captain, A.B. Hungria, P.A. Midgley, R. Raja, J.M. Thomas, Angew. Chem. Int. Ed. 46 (2007) 8182–8185.
[6] A.B. Hungria, R. Raja, R.D. Adams, B. Captain, J.M. Thomas, P.A. Midgley, V. Golvenko, B.F.G. Johnson, Angew. Chem. Int. Ed. 45 (2006) 4782–4785.
[7] R.D. Adams, D.A. Blom, B. Captain, R. Raja, J.M. Thomas, E. Trufan, Langmuir 24 (2008) 9223–9226.
[8] J.M. Thomas, R.D. Adams, E.M. Boswell, B. Captain, H. Grönbeck, R. Raja, Faraday Discuss. 138 (2008) 301–315.
[9] H.C. Clark, G. Ferguson, M.J. Hampden-Smith, H. Ruegger, B.L. Ruhl, Can. J. Chem. 66 (1988) 3120–3127.
[10] L. Vaska, Acc. Chem. Res. 1 (1968) 336–344.
[11] M.F. Lappert, N.F. Travers, Chem. Commun. (1968) 1569–1570.
[12] G. Wittig, F.J. Meyer, G. Lange, Liebigs Ann. Chem. 571 (1951) 167–201.

[13] SAINT+, version 6.2a. Bruker Analytical X-ray Systems, Inc., Madison, WI, 2001.
[14] G.M. Sheldrick, SHELXTL, version 6.1. Bruker Analytical X-ray Systems, Inc., Madison, WI, 1997.
[15] (a) R.D. Adams, E. Trufan, Organometallics 29 (2010) 4346–4353;
(b) M.A. Esteruelas, A. Lledos, O. Maresca, M. Olivan, E. Onate, M.A. Tajada, Organometallics 23 (2004) 1453–1456;
(c) S.W. Lee, K. Yang, J.A. Martin, S.G. Bott, M.G. Richmond, Inorg. Chim. Acta 232 (1995) 57–62.
[16] L. Vaska, J. Am. Chem. Soc. 88 (1966) 4100–4101.
[17] J.M. Allen, W.W. Brennessel, C.E. Bus, J.E. Ellis, M.E. Minyaev, M. Pink, G.F. Warnock, M.L. Winzenburg, V.G. Young Jr., Inorg. Chem. 40 (2001) 5279–5284.
[18] M.A. Esteruelas, F.A. Lahoz, M. Olovan, E. Onate, L.A. Oro, Organometallics 13 (1994) 4246–4257.